

The Hauser-Feshbach calculations for the 1097- and 1189-keV levels in cobalt, gave the results presented by the solid curves on Fig. 5(b). The agreement is reasonable.

The three most abundant isotopes of Zn, comprising more than 95% of natural zinc, have 2^+ excited states at 990, 1040, and 1080 keV. The combined cross sections, for excitation of any of the three levels, are shown on Fig. 5(a). The solid and dashed curves in this figure have the same meaning as above. In this case the measured cross sections strongly favor the Hauser-Feshbach values. This result is difficult to reconcile with current ideas about neutron width distributions. Previous in-

vestigations^{20,22} of Zr^{90} and Fe^{56} have in fact indicated the importance of the width fluctuation for even nuclei.

ACKNOWLEDGMENTS

The authors are indebted to the members of the Applied Nuclear Physics Section for their assistance and to Dr. Peter Moldauer for fruitful discussions. Two of the authors (C. A. Engelbrecht and D. Reitmann) wish to thank the Laboratory Director, Dr. A. V. Crewe, for the hospitality enjoyed at Argonne National Laboratory and also the South African Atomic Energy Board for the opportunity to carry out this work during their overseas tours of duty.

$Fe^{54}(d,p)Fe^{55}$ Reaction and the Nuclear Structure of Ti^{51} , Cr^{53} , and $Fe^{55}\dagger$

JAMES R. MAXWELL* AND W. C. PARKINSON

Department of Physics, Cyclotron Laboratory, The University of Michigan, Ann Arbor, Michigan

(Received 17 February 1964)

Energy levels in Fe^{55} have been investigated by means of the $Fe^{54}(d,p)Fe^{55}$ reaction using 7.8-MeV deuterons from The University of Michigan 42-in. cyclotron. Twenty-eight levels were found up to 5.4 MeV of excitation and angular distributions obtained for eighteen of them. The ℓ_n values and reduced widths were extracted from the data by means of a distorted-wave Born-approximation analysis. An attempt is made to understand the spectra of the 29-neutron nuclei Ti^{51} , Cr^{53} , and Fe^{55} in terms of a shell-model description involving configurations of 2, 4, or 6 ($1f_{7/2}$) protons and a single neutron in the $2p_{3/2}$, $2p_{1/2}$, or $1f_{5/2}$ orbit.

I. INTRODUCTION

THE nuclei Ti^{51} , Cr^{53} , and Fe^{55} form an interesting series because each has 29 neutrons with the last neutron and 2, 4, or 6 protons, respectively, outside of a closed-shell core having the structure of the nucleus Ca^{48} . The interest arises because the spectrum of Ca^{49} as observed in the (d,p) reaction appears to be a pure single-particle spectrum with only three energy levels below an excitation of 3.6 MeV, corresponding to the capture of the neutron into a pure $2p_{3/2}$, $2p_{1/2}$, or $1f_{5/2}$ orbit.¹ In contrast to the situation in Ca^{49} , the spectra of Ti^{51} , Cr^{53} , and Fe^{55} are more complex, there being from six to eight odd parity levels below 4 MeV.²⁻⁸

This paper concerns the properties of energy levels in Fe^{55} which have been studied experimentally by means of the $Fe^{54}(d,p)Fe^{55}$ reaction and the nuclear structure of Ti^{51} , Cr^{53} , and Fe^{55} .

Thin isotopically enriched targets of Fe^{54} were bombarded with 7.8-MeV deuterons from The University of Michigan 42-in. cyclotron and the outgoing protons analyzed with an over-all resolution of 20 keV using a double focusing magnetic spectrometer. Twenty-eight levels were observed up to an excitation of 5.4 MeV in Fe^{55} , and angular distributions were obtained for eighteen of them in the angular range 10° to 60° at 5° intervals and at 70° and 80° . The remaining ten levels were all of very low cross section. Excitation energies were measured and ℓ_n values and reduced widths extracted from the data by means of a distorted-wave analysis.

Since the low-lying levels of the even nuclei Ti^{50} , Cr^{52} , and Fe^{54} are apparently described rather well in terms of the 2, 4, or 6 ($1f_{7/2}$) protons outside of the Ca^{48} core,⁹ it was thought that the level structure of the odd- A nuclei might be understood on the basis of a simple shell-model description in which the 29th neutron in the $2p_{3/2}$, $2p_{1/2}$, or $1f_{5/2}$ orbit is coupled to the possible states of 2, 4, or 6 protons in the $1f_{7/2}$ shell. The results of the shell-model calculation for Ti^{51} , Cr^{53} ,

[†] Supported in part by the U. S. Atomic Energy Commission.

* Present address: School of Physics, University of Minnesota, Minneapolis, Minnesota.

¹ E. Kashy, A. Sperduto, H. A. Enge, and W. W. Buechner, *Bull. Am. Phys. Soc.* **7**, 315 (1962).

² K. Ramavataram, *Bull. Am. Phys. Soc.* **8**, 367 (1963).

³ K. Ramavataram, *Phys. Rev.* **132**, 2255 (1963).

⁴ J. Bardwick, R. S. Tickle, and W. C. Parkinson, *Bull. Am. Phys. Soc.* **8**, 366 (1963).

⁵ J. Bardwick, Ph.D. thesis, The University of Michigan, 1964 (to be published).

⁶ P. T. Andrews, R. W. Clift, L. L. Green, and J. F. Sharpey-Schafer, University of Liverpool Report, 1963 (unpublished).

⁷ A. Sperduto and J. Rapaport, Massachusetts Institute of Technology Laboratory for Nuclear Science Progress Report, 1961 (unpublished).

⁸ R. H. Fulmer and A. L. McCarthy, *Phys. Rev.* **131**, 2133 (1963).

⁹ I. Talmi, *Phys. Rev.* **126**, 1096 (1962).

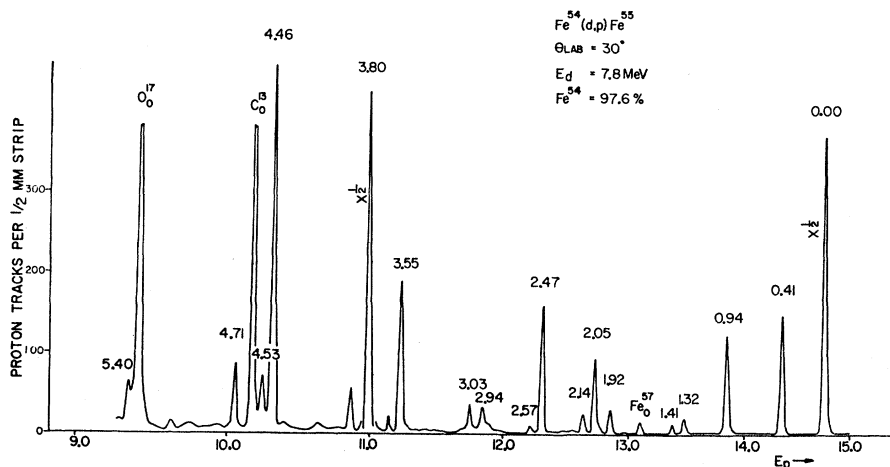


FIG. 1. Fe⁵⁴(d,p)Fe⁵⁵ proton spectrum at 30°.

and Fe⁵⁵ are found to be in good agreement with experiment for levels lying below an excitation of about 2 MeV. Above 2 MeV the model is inadequate.

II. EXPERIMENTAL TECHNIQUES AND RESULTS

The instrumentation associated with The University of Michigan 42-in. cyclotron has been described previously.¹⁰ Briefly, 7.8-MeV deuterons from the cyclotron are magnetically focused onto a 2-mm×10-mm vertical slit placed 5 cm in front of the target in the scattering chamber. Protons from the (d,p) reaction are analyzed in energy with a double focusing magnetic spectrometer which can be moved through the angular range -10° to +95°. The over-all resolution of the beam preparation and analyzer system is about 20 keV. The reaction protons are detected by 1-in. by 10-in. nuclear emulsions placed at the image surface of the analyzer. A Faraday cup and current integrator are used to monitor the beam current. A solid-state detector mounted at 90° to the deuteron beam monitors the elastically scattered deuterons from the target and target backing and is used at low angles in place of the Faraday cup which must be removed for reaction angles less than 30°.

The targets were prepared by evaporating metallic iron isotopically enriched to 97.6% in Fe⁵⁴, the remainder being almost entirely Fe⁵⁶,¹¹ onto thin backings of carbon or gold leaf. Targets with carbon backings, about 50 μg/cm² thick, were used for the measurements except in the regions of excitation where the levels of carbon interfere with those in Fe⁵⁵. In those regions targets with gold leaf backings were used.

The proton spectrum obtained at a scattering angle of 30° from the Fe⁵⁴(d,p)Fe⁵⁵ reaction is shown in Fig. 1. Protons corresponding to the ground-state transition have an energy of about 14.8 MeV, consistent with the known *Q* value of 7.084 MeV.⁷ The

identification of proton groups belonging to Fe⁵⁵ was made from the proton energy-angle kinematics. The levels in Fe⁵⁷, due to the 2.4% Fe⁵⁶ in the target, were identified by checking the relative intensities of levels observed using targets of natural isotopic abundance and targets enriched in Fe⁵⁴. Absolute *Q* values were not measured because the energy of the deuteron beam was not accurately known. However the excitation energies are believed to be accurate within approximately ±20 keV. The uncertainty arises primarily from the variation in the deuteron energy which may be as much as ±10 keV. There is an additional statistical uncertainty of about ±5 keV in locating the position of the proton peak on the plate.

The angular distributions for the eighteen levels in Fe⁵⁵ obtained in the angular range from 10° to 80° are shown in Fig. 2. The relative cross sections are believed to be accurate to within 10%, the principal uncertainties being due to statistical uncertainty in the number of protons observed and indeterminate systematic errors. Absolute cross sections are believed to be accurate only to within about 40%, the uncertainty being due almost entirely to difficulty in obtaining an accurate determination of the target thickness.

While the angular distribution for the 2.05-MeV level includes the 0.367-MeV level in Fe⁵⁷ which could not be resolved, from the target enrichment and a comparison of the Fe⁵⁵ and Fe⁵⁷ spectra it was concluded that the observed cross section is due almost entirely to the level in Fe⁵⁵. The angular distribution for the level at 2.94 MeV includes the contribution from the 1.266-MeV level in Fe⁵⁷ which is known to be an *ℓ_n* = 1 transition¹² and may be the cause for the little structure that is observed in the angular distribution.

The differential cross sections for the remaining ten levels are small, and angular distributions for them were not obtained. The cross sections for the levels at 2.21, 2.30, 2.89, 3.10, 4.02, and 5.12 MeV are less than

¹⁰ D. R. Bach, W. J. Childs, R. W. Hockney, P. V. C. Hough, and W. C. Parkinson, Rev. Sci. Instr. 27, 516 (1956).

¹¹ Obtained from Isotopes Division, ORNL, Oak Ridge, Tennessee.

¹² A. Sperduto, Massachusetts Institute of Technology Laboratory for Nuclear Science Progress Report, 1962 (unpublished).

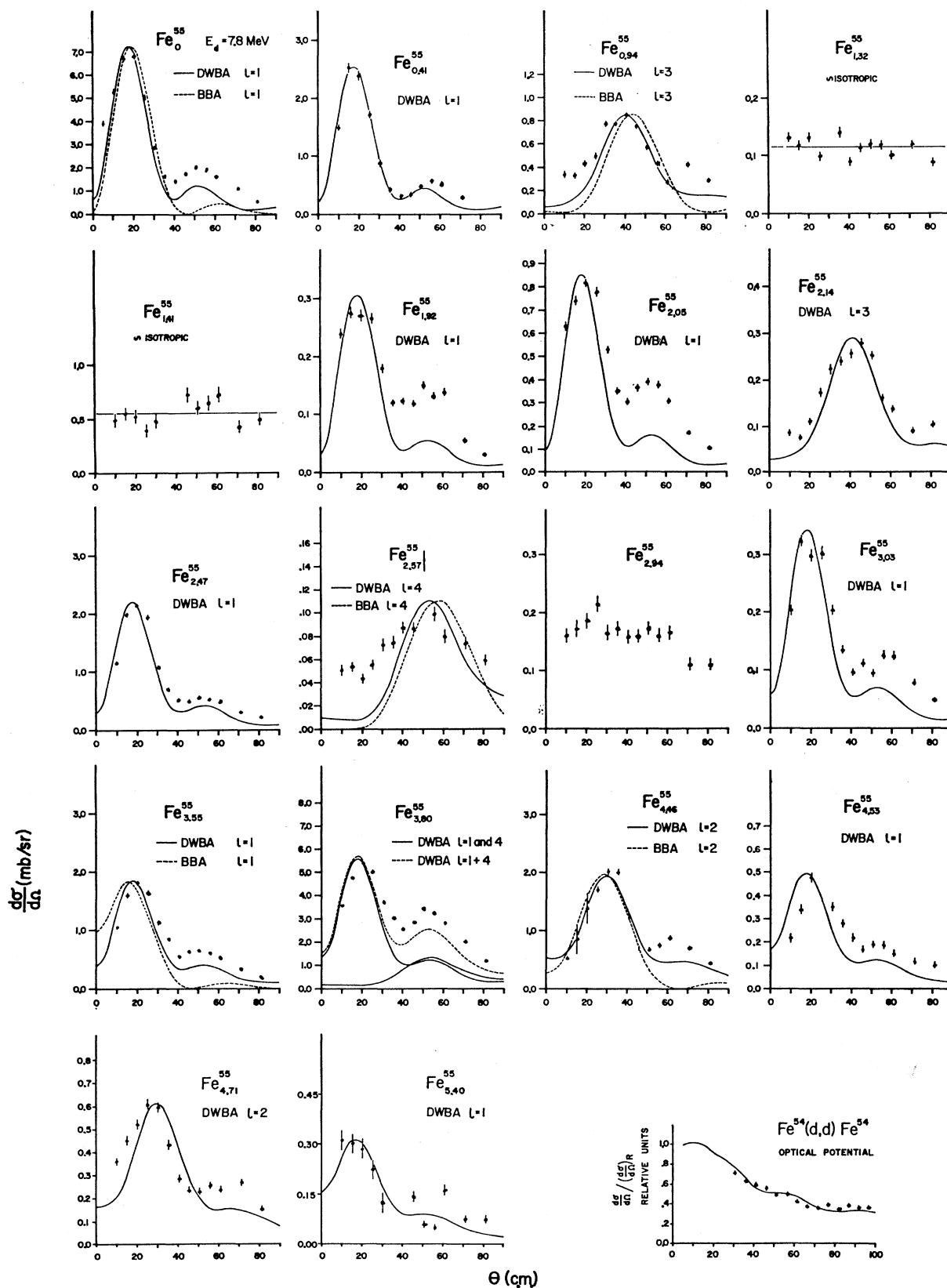


FIG. 2. $Fe^{54}(d,p)Fe^{55}$ and elastic scattering angular distributions.

about 0.1 mb/sr at all angles from 10° to 80°, and for the level at 4.12 MeV may be as large as 0.2 mb/sr at some angles. While there are indications of levels at 2.98 and 4.50 MeV, their cross sections are less than about 0.1 mb/sr and they were not resolved from the stronger levels at 2.94 and 3.03 MeV and at 4.46 and 4.53 MeV. In the region of the spectrum from 4.71 to 5.40 MeV there appear to be several weak levels in Fe⁵⁵, but only the level at 5.12 MeV could be resolved. The angular distribution for the 3.91-MeV level could not be obtained because an impurity proton group masked the level below 35°. Above 35° the cross section was less than about 0.1 mb/sr.

The solid curves shown in Fig. 2 together with the experimental data are the differential cross sections predicted by the DWBA program of Gibbs and Tobocman developed at Rice University and modified at Los Alamos by Rodberg, Swartz, and Hall. The program has been adapted to The University of Michigan IBM-7090 computer⁵ and was used in the analysis of the data. The optical potential parameters were obtained from proton and deuteron elastic-scattering data. The differential cross section for the elastic scattering of 7.8-MeV deuterons from Fe⁵⁴ is shown in Fig. 2. The experimental points are the ratio of the measured cross section to the Rutherford cross section in relative units. The solid curve is the predicted ratio, suitably normalized, calculated with the deuteron optical potential parameters used to fit the Cr⁵² deuteron elastic-scattering data.⁵ Since the agreement was considered quite reasonable no attempt was made to vary the parameters for a "best fit." The proton optical potential parameters are those used by Andrews *et al.* to fit the Cr⁵³(p, p)Cr⁵³ data at 10 MeV.¹³ In several of the figures Butler curves (BBA) are shown for comparison. They were calculated by the computer program using a cutoff radius $r_0=5.8$ F with the Coulomb and optical potentials set equal to zero.

In computing the reduced widths the radius R_N , the radius at which the bound-state harmonic oscillator and exponentially decaying neutron wave functions are matched, was chosen as 6.60 F for Fe⁵⁵ since the absolute (d, p) cross section for the Ca⁴⁸(d, p)Ca⁴⁹ ground-state transition is correctly predicted using $R_N=6.65$ F.¹⁴ This is known to be a pure $2p_{3/2}$ transition for which the spectroscopic factor is unity.

The excitation energies, ℓ_n values, and spectroscopic factors $(2J+1)S$ determined from the distorted wave theory are given in Table I together with the relative reduced widths $(2J+1)\theta^2$ obtained from the Butler theory.

The sum of the $(2J+1)S$ factors for all of the $\ell_n=1$ transitions is equal to 3.99 and includes fragments of

¹³ P. T. Andrews, R. W. Clift, L. L. Green, and J. F. Sharpey-Schafer, University of Liverpool Report, ULDP-12, 1961 (unpublished).

¹⁴ F. P. Gibson and E. Kashy, Massachusetts Institute of Technology Laboratory for Nuclear Science Progress Report, 1962 (unpublished).

TABLE I. A summary of experimental results.

Exc (MeV)	ℓ_n	DWBA (2J+1)S	DWBA (2J+1)S relative	BBA (2J+1) θ^2 relative $r_0=5.8$ F
0.00	1	1.84	4.00	4.00
0.41	1	0.61	1.32	1.37
0.94	3	2.11	4.59	2.63
1.32	\sim iso ^a
1.41	\sim iso
1.92	1	0.05	0.11	0.14
2.05	1	0.14	0.31	0.39
2.14	3	0.53	1.15	0.85
2.21
2.30
2.47	1	0.32	0.70	0.98
2.57	4	0.47	1.02	0.66
2.89
2.94	\sim iso
2.98
3.03	1	0.05	0.10	0.14
3.10
3.55	1	0.23	0.49	0.71
	{	0.67	1.46	2.05
3.80	{(4)	4.65	10.11	...
3.91
4.02
4.12
4.46	2	0.47	1.02	2.03
4.50
4.53	1	0.05	0.12	0.16
4.71	2	0.14	0.31	0.62
5.12
5.40	1	0.03	0.07	0.09

^a Approximately isotropic.

both the $2p_{3/2}$ and $2p_{1/2}$ single-particle levels. If no $\ell_n=1$ transitions have been missed in the experiment the sum should be equal to 6. It is unlikely that so much $2p$ strength has been missed in the region of excitation below 5.4 MeV, and unlikely that it should occur above 5.4 MeV. The measured absolute cross sections may be too small, or the distorted wave theory may overestimate the cross sections.

The fits to the angular distributions appear to be very good. The $\ell_n=1$ levels are probably fragments of the $2p_{3/2}$ and $2p_{1/2}$ levels, and the $\ell_n=3$ levels fragments of the $1f_{5/2}$ level. The $\ell_n=2$ transition at 4.46 MeV seems to be the first indication of the $2d_{5/2}$ level. A weak $\ell_n=4$ level at 2.57 MeV is probably a fragment of the $1g_{9/2}$ level.

The level at 3.80 MeV is an $\ell_n=1$ transition but the second maximum in the angular distribution is unusually large compared, for example, to the angular distribution for the 3.55-MeV level. An $\ell_n=4$ level may give rise to the large secondary maximum, but an admixture of ℓ_n values is forbidden. If the level is a doublet, the splitting would have to be less than 10 keV because no change in shape of the proton peak was observed at the various angles. If there is an $\ell_n=4$ level at 3.80 MeV it would appear to have a spectroscopic factor $(2J+1)S=4.65$. This is reasonable from the systematics in this mass region.

The very weak levels at 1.32 and 1.41 MeV do not

show characteristic stripping angular distributions. These are discussed further in Sec. III.

The Butler reduced widths were obtained with a fixed cutoff radius $r_0=5.8$ F. For the $\ell_n=1$ transitions these reduced widths become larger relative to the distorted-wave reduced widths for levels at higher excitations. They would become even larger if the Butler reduced widths were evaluated using a "best fit" radius, which tends toward 4.0 F for levels at higher excitations.

The excitation energies, ℓ_n values, and reduced widths that have been obtained are in good agreement with previous results. The 4.46-MeV level has been assigned an $\ell_n=2$, rather than $\ell_n=1$ as in Ref. 7, and there appears to be an $\ell_n=4$ level at 3.80 MeV as in Ref. 8. Several levels observed in Ref. 7 were not seen due to their small cross sections.

III. A SHELL-MODEL INTERPRETATION OF THE LOW-LYING LEVELS IN Ti^{51} , Cr^{53} , AND Fe^{55}

The low-lying negative-parity levels observed in the (d,p) reaction in the nuclei Ti^{51} , Cr^{53} , and Fe^{55} are presumably fragments of the $2p_{3/2}$, $2p_{1/2}$, and $1f_{5/2}$ neutron single-particle levels. In Fe^{55} the single-particle strengths are clearly not concentrated in the first three levels, but are shared with many of the higher excited states. The situation is much the same in Ti^{51} and Cr^{53} .²⁻⁶ One would like to understand the fragmentation of the single-particle states and the level structure in these nuclei on the basis of a model of the nucleus.

Talmi has shown that the energies and $M1$ transition rates for Cr^{52} agree rather well with that expected for a $(1f_{7/2})^4$ proton configuration when proton-proton interactions are included.⁹ It was therefore thought that the odd- A nuclei Ti^{51} , Cr^{53} , and Fe^{55} might be understood on the basis of a shell-model description in which a neutron in the $2p_{3/2}$, $2p_{1/2}$, or $1f_{5/2}$ level is coupled to the possible core states of 2, 4, or 6 protons in the $1f_{7/2}$ shell.

The validity of such a model might be expected to extend to only 2 or 3 MeV because of evidence that other core excitations become important above this excitation. For example, the results of a $\text{Mn}^{55}(p,\alpha)\text{Cr}^{52}$ measurement seem to require a seniority mixing of the two $J=4$ levels in Cr^{52} suggesting the possible importance of levels involving a proton excitation out of the $1f_{7/2}$ shell or excitation of the Ca^{48} core.¹⁵ The $\text{Fe}^{56}(p,d)\text{Fe}^{55}$ experiment indicates an $\ell_n=3$ neutron pick up at 1.4 MeV in Fe^{55} . This is presumably a spin- $\frac{7}{2}$ level involving a configuration in which a $1f_{7/2}$ neutron has been excited.¹⁶ Since such excitations have not been included in the present model good agreement cannot be expected even for the lowest spin- $\frac{7}{2}$ levels. Hopefully, however, the low-lying levels with spins $\frac{1}{2}$, $\frac{3}{2}$, and $\frac{5}{2}$, which are of greatest interest in the (d,p)

experiments, do not involve such excitations since levels with spins different from $\frac{7}{2}$ involving a neutron excitation out of the closed $1f_{7/2}$ neutron shell might be expected to lie higher in energy.

The shell-model wave functions for the nuclei Ti^{51} , Cr^{53} , and Fe^{55} are taken to be angular momentum coupled-properly antisymmetrized products of single-particle harmonic-oscillator wave functions of the form

$$\Psi_{JM^0}(J_n, j) = |(\pi 1f_{7/2})^n J_n, \nu n l j; JM\rangle.$$

Antisymmetry in the proton wave function (π) is assured by restricting the spin $J_n=0$ ($\nu_n=0$), or $J_n=2$, 4, or 6 ($\nu_n=2$) in Ti^{51} and Fe^{55} , or in addition $J_n=2$, 4, 5, or 8 ($\nu_n=4$) in Cr^{53} . The odd neutron (ν) is in orbits $n l j$ different from $1f_{7/2}$ so that the wave functions do not have to be antisymmetrized in the neutron-proton coordinates for the evaluation of the interaction energy.

The neutron single-particle energies are taken from the experimental data for Ca^{49} . The $(2p_{1/2}-2p_{3/2})$ energy difference is 2.03 MeV, and the $(1f_{5/2}-2p_{3/2})$ energy difference is 3.59 MeV. The degeneracy of states of various proton spin J_n of the configuration $(\pi 1f_{7/2})^n$ is removed by the residual proton-proton interaction. The matrix elements for the proton-proton interaction have been taken from the experimentally observed level splittings in the neighboring even nuclei.

A neutron-proton interaction removes the degeneracy of states with the same J_n and j but different total spin J . The neutron-proton interaction potential was chosen with a Gaussian radial dependence

$$V_{\nu\pi} = V_0 e^{-r_\nu r_\pi^2 / r_0^2} (W + B P_\sigma + H P_\sigma P_\tau + M P_\tau)$$

and a range $r_0 \simeq 2.8$ F, corresponding to a range parameter $\lambda^2=1$ where $\lambda^2 = m\omega/2\hbar r_0^2$. The frequency of the harmonic oscillator well, ω , is given by $\hbar\omega \simeq 41A^{-1/3}$ MeV. The P_σ and P_τ are the spin exchange and space exchange operators. The coefficients W , B , H , and M give the strength of the various exchange potentials.

Several different exchange mixtures have been used in various shell-model calculations.¹⁷⁻²⁰ For the present calculation the Serber exchange mixture, $W=M=0.5$, $B=H=0$ with a well depth $V_0=-40$ MeV, and a Serber-like exchange mixture, $W=M=0.4$, $B=0.2$, $H=0$ with $V_0=-40$ MeV, were found to give quite reasonable results. No attempt was made to vary the neutron-proton interaction potential for a "best fit" to the data.

The dimensions of the interaction matrices for the spin- $\frac{1}{2}$, $\frac{3}{2}$, and $\frac{5}{2}$ states are 3×3 , 5×5 , and 6×6 , respectively, in Ti^{51} and Fe^{55} , and 5×5 , 9×9 , and 12×12 in Cr^{53} . The diagonalization was carried out on the University of Michigan IBM-7090 computer for the

¹⁷ J. P. Elliott and B. H. Flowers, Proc. Roy. Soc. (London) **A229**, 536 (1955).

¹⁸ S. Meshkov and C. W. Ufford, Phys. Rev. **101**, 734 (1956).

¹⁹ B. H. Flowers, *Proceedings of the Rehovoth Conference on Nuclear Structure*, edited by H. J. Lipkin (North-Holland Publishing Company, Amsterdam, 1958), p. 17.

²⁰ E. H. Schwarcz, Phys. Rev. **129**, 727 (1963).

¹⁵ B. F. Bayman, Bull. Am. Phys. Soc. **8**, 80 (1963).

¹⁶ C. D. Goodman, J. B. Ball, and C. B. Fulmer, Phys. Rev. **127**, 574 (1962).

energies and wave functions. The final wave functions are of the form

$$\Psi_{JM} = \sum_{J_n, i} \alpha_{J_n, i} \Psi_{JM}^0(J_n, j).$$

The coefficient $(\alpha_{J=j}^{J_n=0, i})^2$ is just the predicted spectroscopic factor S in the reduced width for a (d, p) transition to a fragment of the single-particle level j .

The matrix elements that have to be evaluated are of the form

$$\langle (\pi 1 f_{7/2})^n J_n', \nu n' l' j'; JM | \sum_{i=1}^n V_{\pi v_i} | (\pi 1 f_{7/2})^n J_n, \nu n l j; JM \rangle.$$

These matrix elements can be reduced to sums of two-particle matrix elements by the standard techniques of Racah²¹ to

$$n \sum_{J_3} (-1)^{i'+i+1} (2J_3+1) [(2J_n'+1)(2J_n+1)]^{1/2} \times \left[\sum_{j'} \left\{ \begin{matrix} g & 7/2 & J_n' \\ j' & J & J_3 \end{matrix} \right\} \left\{ \begin{matrix} g & 7/2 & J_n \\ j & J & J_3 \end{matrix} \right\} \langle (7/2)^n (\nu n' J_n') | \right] \times \left[\sum_{j} \left\{ \begin{matrix} g & 7/2 & J_n \\ j & J & J_3 \end{matrix} \right\} \langle (7/2)^n (\nu n J_n) | \right] \times \langle (7/2)^{n-1} g | \langle (7/2)^n (\nu n J_n) | \rangle \langle (7/2)^{n-1} g \rangle \times \langle 7/2 j' J_3 M_3 | V_{\pi \pi} | 7/2 j J_3 M_3 \rangle.$$

The coefficients of fractional parentage $\langle (j)^n (\nu n J_n) | \rangle \times \langle (j)^{n-1} (\nu_{n-1} J_{n-1}) \rangle$ have been tabulated by Edmonds and Flowers.²² The 6- j coefficients $\left\{ \begin{matrix} j_1 & j_2 & J_{12} \\ j_3 & J & J_{23} \end{matrix} \right\}$ are taken from the tables of Rotenberg *et al.*²³ The two-particle matrix elements have been evaluated using the general techniques of Talmi²⁴ and Brody and Moshinsky.²⁵

The quantities of greatest interest, to be compared with the experimental results for the three nuclei Ti⁵¹, Cr⁵³, and Fe⁵⁵, are the energies, the spins, and the spectroscopic factors for the various levels. Analysis of the measured differential cross sections, however, yields values of the orbital angular momentum ℓ_n of the captured neutron and the product $(2J+1)S$. Since the value of J for some of the levels is uncertain, $(2J+1)S$ is used to compare the predicted and observed reduced widths. The spectroscopic factors S have been normalized to unity for the ground-state transitions for ease

²¹ G. Racah, Phys. Rev. **62**, 438 (1942); **63**, 367 (1943); and **76**, 1352 (1949). The general techniques of Racah are presented by A. de Shalit and I. Talmi in *Nuclear Shell Theory* (Academic Press Inc., New York, 1963).

²² A. R. Edmonds and B. H. Flowers, Proc. Roy. Soc. (London) **A214**, 515 (1952).

²³ M. Rotenberg, R. Bivins, N. Metropolis, and J. K. Wooten, Jr., *The 3-j and 6-j Symbols* (The Technology Press, Cambridge, Massachusetts, 1959).

²⁴ I. Talmi, Helv. Phys. Acta **25**, 185 (1952).

²⁵ T. A. Brody and M. Moshinsky, *Tables of Transformation Brackets* (Monografias del Instituto de Fisica, Mexico City, 1960), and references therein.

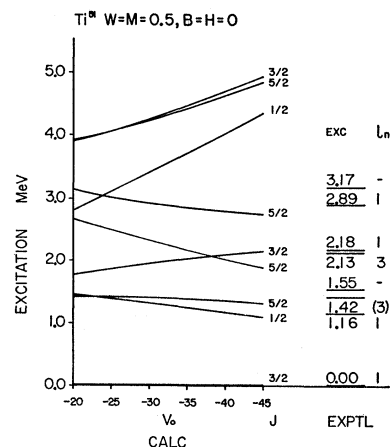


FIG. 3. The spectrum calculated for Ti⁵¹ using a Serber exchange mixture and $V_0 = -20$ MeV to -45 MeV with the experimental spectrum.

of comparison. The ground-state magnetic moment and quadrupole moment as well as one transition probability for Cr⁵³ have been measured²⁶⁻²⁸ and are also used in comparing the theory with experiment.

A. Results for Ti⁵¹

The predicted energy levels and spins for Ti⁵¹ are shown in Fig. 3 as a function of the well depth V_0 for a Serber exchange mixture together with the experimentally observed levels and ℓ_n values.^{2,3} The predicted spin- $\frac{1}{2}$ and spin- $\frac{3}{2}$ levels are fragments of the $2p_{1/2}$ and $2p_{3/2}$ neutron single-particle levels and correspond to the $\ell_n=1$ transitions observed in the (d, p) measurement, while the spin- $\frac{5}{2}$ levels are fragments of the $1f_{5/2}$ level corresponding to the levels with $\ell_n=3$ angular distributions. The spectrum calculated for $V_0 = -40$ MeV is very nearly the same as that observed experimentally.

The spectrum calculated for $V_0 = -40$ MeV using the Serber exchange mixture is shown in Fig. 4 including

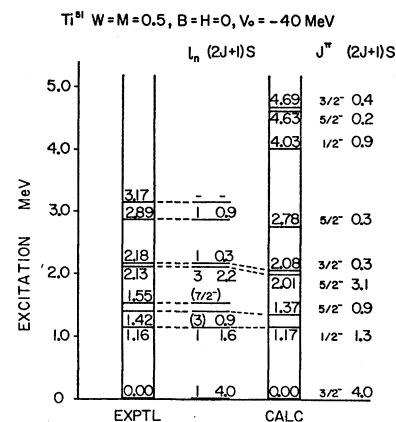


FIG. 4. The spectrum calculated for Ti⁵¹ using a Serber exchange mixture and $V_0 = -40$ MeV with the experimental spectrum.

²⁶ *Nuclear Data Sheets*, compiled by K. Way *et al.* (Printing and Publishing Office, National Academy of Sciences, National Research Council, Washington 25, D. C.).

²⁷ R. W. Terhune, J. Lambe, C. Kikuche, and J. Baker, Phys. Rev. **123**, 1265 (1961).

²⁸ E. C. Booth and K. A. Wright, Bull. Am. Phys. Soc. **8**, 85 (1963).

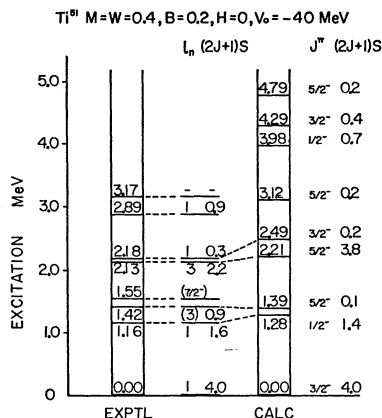


FIG. 5. The spectrum calculated for Ti^{61} using $W=M=0.4, B=0.2, H=0$ and $V_0=-40$ MeV with the experimental spectrum.

only remaining level below 3 MeV, at 1.55 MeV, is very weak and shows an isotropic angular distribution in (d,p) stripping. It is believed to be a spin- $\frac{7}{2}$ level^{2,3} arising out of the configuration

$$[(\pi 1 f_{7/2})^2 J_2 = 2, \nu 2 p_{3/2}; J = \frac{7}{2}]$$

with a predicted spectroscopic factor of zero.

The effect of varying the exchange parameters for the two-body interaction on the predicted spectrum of Ti^{61} is illustrated in Fig. 5. The exchange mixture $W=M=0.4, B=0.2, H=0$ was used with $V_0=-40$ MeV. The spin sequence for the various levels is not altered but the over-all fit to the experimental data is somewhat less satisfactory than for the Serber force.

B. Results for Cr^{53}

The same exchange mixtures and well depth for the neutron-proton interaction were used for Cr^{53} as for Ti^{61} . The spectrum calculated with the Serber exchange

energies, spins, and relative reduced widths $(2J+1)S$. The agreement with experiment for levels up to about 2 MeV is seen to be very reasonable. The ground-state spin of Ti^{61} has not been measured, but it is expected to be $\frac{3}{2}$. The level predicted at 1.17 MeV with $J=\frac{1}{2}$ and $(2J+1)S=1.3$ presumably corresponds to the level observed at 1.16 MeV with $l_n=1$ and $(2J+1)S=1.6$. The level at 1.42 MeV may be an $l_n=3$ but is weak and the $l_n=3$ assignment is tentative. The $(2J+1)S$ is estimated to be about 0.9. The model predicts a very weak $J=\frac{5}{2}$ level at 1.37 MeV with $(2J+1)S=0.9$. A strong $l_n=3$ transition is observed at 2.13 MeV with $(2J+1)S=2.2$ and appears to correspond to the level predicted at 2.01 MeV with $J=\frac{5}{2}$ and $(2J+1)S=3.1$. A weak $l_n=1$ transition at 2.18 MeV with $(2J+1)S=0.3$ presumably corresponds to the $J=\frac{3}{2}$ level predicted at 2.08 MeV with $(2J+1)S=0.3$. While no other spin- $\frac{1}{2}$ or spin- $\frac{3}{2}$ levels are predicted below 4 MeV, an $l_n=1$ transition with $(2J+1)S=0.9$ is observed at 2.89 MeV. A $J=\frac{1}{2}$ level is predicted, however, at an excitation of 4.03 MeV with $(2J+1)S=0.9$ and is the only $l_n=1$ transition above about 2 MeV predicted to have this much strength. It is thus believed to correspond to the 2.89-MeV level, and while it is predicted to be at too high an energy, it might possibly be depressed if higher core excitations were included in the calculation. The

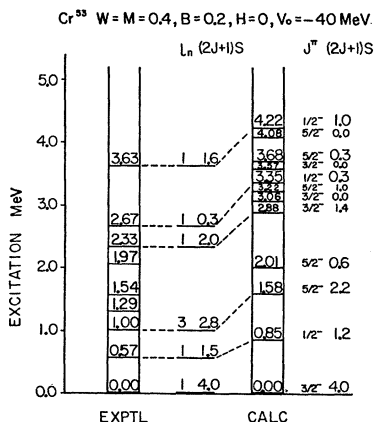


FIG. 7. The spectrum calculated for Cr^{53} using $W=M=0.4, B=0.2, H=0$ and $V_0=-40$ MeV with the experimental spectrum.

mixture and $V_0=-40$ MeV is shown in Fig. 6 together with the (d,p) experimental data.⁴⁻⁶ The results with $W=M=0.4, B=0.2, H=0$ and $V_0=-40$ MeV are shown in Fig. 7. The spins and parities for a number of levels in Cr^{53} have been measured by Van Patter *et al.*²⁹ and by Bartholomew and Gunye.³⁰ The ground state has $J^\pi = \frac{3}{2}^-$, the 0.57 MeV level $\frac{1}{2}^-$, the 1.00-MeV level $\frac{5}{2}^-$, the 2.33-MeV level $\frac{3}{2}^-$, and the 2.67- and 3.63-MeV levels tentatively $\frac{1}{2}^-$ and $\frac{3}{2}^-$, respectively.

The Serber force with $V_0=-40$ MeV fits the first two excited states quite well. A $J=\frac{1}{2}$ level is predicted at 0.66 MeV with $(2J+1)S=1.1$, and a $J=\frac{5}{2}$ level at 1.08 MeV with $(2J+1)S=2.5$. These levels correspond to the observed $l_n=1$ first excited state and $l_n=3$ second excited state at 0.57 and 1.00 MeV with $(2J+1)S=1.5$ and 2.8, respectively.

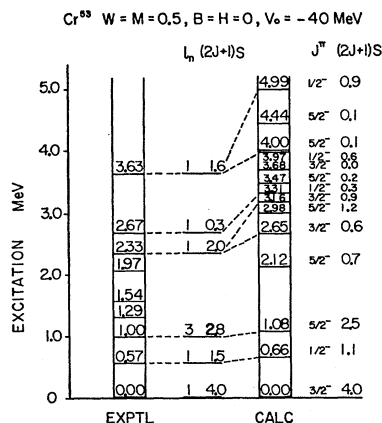


FIG. 6. The spectrum calculated for Cr^{53} using a Serber exchange mixture and $V_0=-40$ MeV with the experimental spectrum.

²⁹ D. M. Van Patter, N. Nath, S. M. Sharfroth, S. S. Malik, and M. A. Rothman, *Phys. Rev.* **128**, 1246 (1962).

³⁰ G. A. Bartholomew and M. R. Gunye, *Bull. Am. Phys. Soc.* **8**, 367 (1963).

One predominant feature of the Cr⁵³ nucleus is the level at 2.33 MeV with $J = \frac{3}{2}$ and $(2J+1)S = 2.0$. This level shares a large part of the $2p_{3/2}$ neutron single-particle strength. There are two $J = \frac{3}{2}$ levels above the ground state predicted with an appreciable reduced width, one at 2.65 MeV with $(2J+1)S = 0.6$ and another at 3.16 MeV with $(2J+1)S = 0.9$, but the combined strength is not as large as is observed experimentally in the 2.33-MeV level. The effect of a slight change in the exchange mixture is to concentrate these strengths into one or the other of these levels, as is seen in Fig. 7, but at the expense of a fit to the first two levels.

The level at 3.63 MeV is difficult to understand as it has tentatively been assigned $J = \frac{3}{2}^{30}$ and has a large reduced width, $(2J+1)S = 1.6$. No comparably strong $\ell_n = 1$ transitions are predicted by the model above 3.2 MeV, although the observed strength is about equal to the sum of the $(2J+1)S$ values of the predicted $J = \frac{1}{2}$ levels at 3.97 and 4.99 MeV (Fig. 6). Then on the basis of the distribution of reduced widths the model would seem to indicate a $J = \frac{1}{2}$ spin assignment for the 3.63-MeV level.

The $\ell_n = 1$ transition observed at 2.67 MeV is a doublet and may have an $\ell_n = 1$ and an $\ell_n = 3$ component.⁶ An $\ell_n = 3$ transition might be expected in this region of excitation in Cr⁵³ and there are several $J = \frac{5}{2}$ levels predicted by the model above 2 MeV.

An explanation of the energy levels in Cr⁵³ in terms of the shell model may involve more complicated excitations of the Cr⁵² core besides those of the $(\pi 1f_{7/2})^4$ configuration. In this connection it should be pointed out that there is an excited state in Cr⁵² at 2.648 MeV tentatively assigned $J = 0^{26}$ which has been ignored in the present shell-model calculation. Since no information is available which would give a clue as to the nature of this excitation, no attempt has been made to incorporate it into the calculation. Possibly this forms the main factor limiting the validity of the model.

The ground-state magnetic moment of Cr⁵³ has been measured to be $\mu = -0.475$ nm.²⁶ The value calculated is -0.98 nm for the ground state using the Serber exchange mixture and $V_0 = -40$ MeV (or -1.05 nm for $W = M = 0.4$, $B = 0.2$, $H = 0$ and $V_0 = -40$ MeV). This is a considerable improvement over the single-particle Schmidt value of -1.913 nm but is not in strikingly good agreement with the observed value of -0.475 nm.

The static quadrupole moment for the Cr⁵³ ground state has been measured by Terhune *et al.*²⁷ to be $Q = -0.03$ b. Using the ground-state wave function of Cr⁵³ calculated with the Serber exchange mixture and $V_0 = -40$ MeV, the value predicted is $Q = -0.08$ b. The predicted quadrupole moment is smaller than the single particle value for one $1f_{7/2}$ proton by a factor of about 2, and it is perhaps surprising that the experimental value is even smaller.

The spin of the 2.33-MeV level is $\frac{3}{2}$ and the lifetime $(4 \pm 2) \times 10^{-15}$ sec.²⁸ The radiation is assumed to be

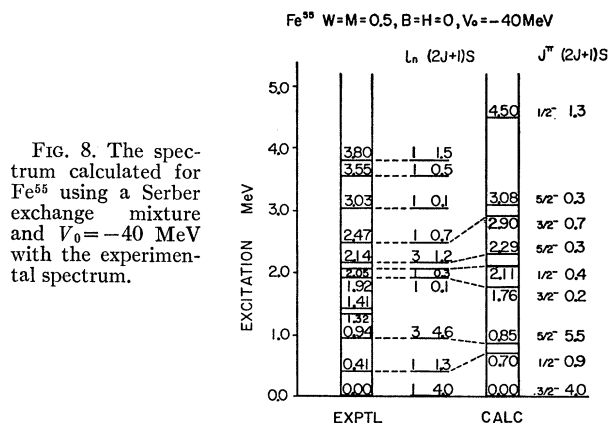


FIG. 8. The spectrum calculated for Fe⁵⁵ using a Serber exchange mixture and $V_0 = -40$ MeV with the experimental spectrum.

mainly $M1$. For a pure $M1$ transition the observed lifetime implies a transition probability of about $\frac{1}{5}$ the single-particle Weisskopf estimate, whereas for $E2$ radiation this lifetime would imply a transition probability of about 200 times the single-particle Weisskopf estimate, much more than the usual collective enhancement observed in other nuclei in this region. The observed lifetime corresponds to a $B(M1)/\mu_N^2 = 1.14$. The value predicted using wave functions for the Serber exchange mixture and $V_0 = -40$ MeV is $B(M1)/\mu_N^2 = 0.03$ which is too small by a factor of about 40, another indication that the 2.33-MeV level is not very well described by the corresponding level at 2.65 MeV in the model.

C. Results for Fe⁵⁵

The spectra of Fe⁵⁵ calculated using the Serber and the $W = M = 0.4$, $B = 0.2$, $H = 0$ mixtures for $V_0 = -40$ MeV are shown in Figs. 8 and 9 together with the (d, p) experimental data. The ground-state spin has been measured to be $\frac{3}{2}$,²⁶ and in addition the preliminary results of Gemmel *et al.*³¹ indicate that the spin of the

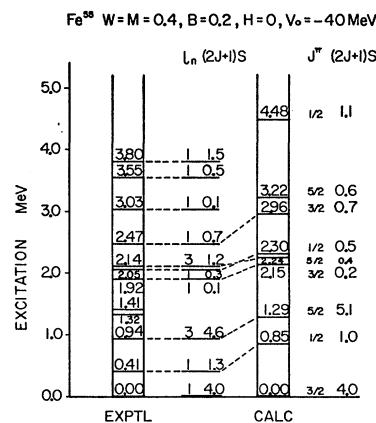


FIG. 9. The spectrum calculated for Fe⁵⁵ using $W = M = 0.4$, $B = 0.2$, $H = 0$ and $V_0 = -40$ MeV with the experimental spectrum.

³¹ D. S. Gemmel, L. L. Lee, Jr., A. Marinov, and J. P. Schiffer, *Bull. Am. Phys. Soc.* **8**, 523 (1963).

0.41-MeV level is $\frac{1}{2}$ and the 2.47- and 3.80-MeV levels $\frac{3}{2}$. The fit to the first two excited states is better with the Serber mixture and $V_0 = -40$ MeV as with Ti^{51} and Cr^{53} although the agreement is semiquantitative at best. The first excited state is predicted at 0.70 MeV with $J = \frac{1}{2}$ and $(2J+1)S = 0.9$, and an $\ell_n = 1$ transition is observed at 0.41 MeV with $(2J+1)S = 1.3$. The second excited state is predicted at 0.85 MeV with $J = \frac{5}{2}$ and $(2J+1)S = 5.5$, and an $\ell_n = 3$ transition is observed at 0.94 MeV with $(2J+1)S = 4.6$. The next $J = \frac{5}{2}$ level is predicted at 2.29 MeV with $(2J+1)S = 0.3$ and corresponds to the $\ell_n = 3$ transition observed at 2.14 MeV with a much larger reduced width, $(2J+1)S = 1.2$. The $J = \frac{3}{2}$ level predicted at 1.76 MeV and the $J = \frac{1}{2}$ level predicted at 2.11 MeV seem to correspond to the $\ell_n = 1$ transitions at 1.92 and 2.05 MeV. A strong $\ell_n = 1$ transition is observed at 2.47 MeV which may correspond to the $J = \frac{3}{2}$ level at 2.90 MeV. Although the preliminary measurements indicate a $J = \frac{3}{2}$ spin assignment for the 3.80-MeV level,³¹ the only $\ell_n = 1$ transition predicted above 3 MeV with comparable strength is the $J = \frac{1}{2}$ level at 4.50 MeV so that on the basis of the distribution of reduced widths the model would favor a $J = \frac{1}{2}$ assignment. The energy and $(2J+1)S$ fits are not in excellent quantitative agreement but the over-all fit to the experimental spectrum is still quite reasonable.

Two levels that have not been discussed in Fe^{55} are those at 1.32 and 1.41 MeV. Both of these levels are very weakly excited in stripping and neither show a stripping type angular distribution, although other (d,p) experiments indicate that the 1.32-MeV level may be an $\ell_n = 3$.^{7,8} No $J = \frac{5}{2}$ level is predicted in this region and the 1.41 MeV level seems to be a $J = \frac{7}{2}$ level arising from a neutron excitation out of the $1f_{7/2}$ shell.¹⁶ The 1.32-MeV level could conceivably be a $J = \frac{7}{2}$ level arising out of the $[(\pi 1f_{7/2})^6 J_6 = 2, \nu 2p_{3/2}; J = \frac{7}{2}]$ configuration although it is perhaps surprising that two $J = \frac{7}{2}$ levels would be so close together.

IV. CONCLUSIONS

Experimentally, twenty-eight levels have been observed in Fe^{55} and the excitation energies as well as the ℓ_n values and spectroscopic factors $(2J+1)S$ obtained. The shell-model description presented in Sec. III seems to account, at least in a qualitative way, for the properties of the low-lying levels in Ti^{51} , Cr^{53} , and Fe^{55} . In all three nuclei the ground state is predicted to have $J = \frac{3}{2}$, the first excited state $J = \frac{1}{2}$, and the second excited state $J = \frac{5}{2}$. The energies and reduced widths compare rather well with the experimentally observed values. The next $\ell_n = 1$ transitions are predicted to be $J = \frac{3}{2}$ levels with several $\frac{3}{2}$, $\frac{1}{2}$, and $\frac{5}{2}$ levels above 2 MeV with appreciable reduced width.

It is of interest to note that the calculation done by Ramavataram^{2,3} for this same series of nuclei, using a unified model in which the 29th neutron is coupled to a collective core, produces similar results but in somewhat better agreement with the experimental data. One of the interesting results obtained using the unified model is that the quadrupole effects seem to be more pronounced in Cr^{53} than in either Ti^{51} or Fe^{55} . This may be a clue as to the difficulty encountered in understanding the structure of Cr^{53} . A better description of these nuclei might be obtained with the shell model if collective effects of the core nucleus Ca^{48} were included.

ACKNOWLEDGMENTS

The authors are particularly grateful to Professor K. T. Hecht for suggesting the possible interpretation of the experimental data and for many stimulating discussions throughout the course of the work. We are grateful to J. Koenig and the cyclotron staff for assistance in running the cyclotron, and to Mrs. Lorraine Graf for developing and scanning the nuclear emulsion plates. Thanks are due to Dr. J. Bardwick who provided the DWBA calculations used in the analysis of the angular distributions, and to Dr. R. Leacock for programming the matrix diagonalization.